# Small Unsteady Perturbations in Transonic Flows

K-Y. Fung,* N. J. Yu,* and R. Seebass†
*University of Arizona, Tucson, Ariz.*

**The effects of very small, low-frequency perturbations on steady transonic flows, in the context of two-dimensional flows described by the small perturbation equation, are investigated. Previous time-linearized studies failed to account for the shock wave motions that are known to occur. A method is provided that allows one to correctly account for shock wave motions due to arbitrary but small unsteady changes in the boundary conditions. Consequently, both harmonic and indicial responses may be determined. Time-linearized results for the transonic flow past an NACA 64A006 airfoil experiencing harmonic motions in one of several modes are presented. Selected results are compared with those obtained from nonlinear calculations using a shock-fitting algorithm.**

## Introduction

IN unsteady transonic flow, relatively small periodic changes in the boundary conditions can lead to substantial changes in the magnitude and phase lag of loads and moments. These are of major concern in the aerodynamic design of aircraft that operate in the transonic regime. Reference 1 contains a short but timely review of various aspects of unsteady transonic flow. Of particular concern are aeroelastic behavior and flutter boundaries. Here the unsteady perturbations may be considered small, and linearization about a nonlinear steady flow, as suggested by Landahl[2] long ago, would seem to be appropriate. Indeed, it has been suggested[3] more recently that the steady flow be determined experimentally. Difficulties arise, however, which detract from this procedure. Although the equation is linear, its coefficients are variable and must be determined by numerical solution of a nonlinear problem that, in the cases of prime interest, has a discontinuous solution; that is, there are embedded shock waves. Also, although a change of variables in the linear equation provides a scaling of parameters which is indicative of the tradeoffs between, e.g., Mach number and reduced frequency, the only similitude is the one basic to the nonlinear formulation.

Traci et al.[4] have developed relaxation methods for solving the resulting time-linearized equations of motion. Less complete but comparable studies have been made by Weatherill et al.[5]; these derive from an earlier study by Ehlers.[6] In both of these studies shock motions, which contribute substantially to the time-varying loads and moments,[7,8] are neglected. Also, difficulties arise in the convergence of the iterative numerical scheme.

Here we pursue a different numerical course. Yu et al.[9] have developed a numerical procedure for computing solutions to the unsteady small perturbation equation for transonic flows which treats embedded shock waves as discontinuities. This procedure can be used to calculate the basic steady flow that we wish to subject to small unsteady perturbations. A simplified version of this algorithm then can be used to calculate the linearized unsteady perturbations to the flow. These calculations can be carried out in conjunction with an algorithm that determines the shock wave motion. The procedure that we have used to calculate the shock wave motion is a rather obvious one; it is not surprising, then, that it, too, was given in the monograph by Landahl[2] (Sec. 10.2). An alternative procedure, related in some ways to that used here, is implied by Nixon's[10] study of perturbations to steady discontinuous transonic flows.

Presented as Paper 77-675 at the AIAA 10th Fluid and Plasmadynamics Conference, Albuquerque, N. Mex., June 27-29, 1977; submitted Nov. 14, 1977; revision received March 15, 1978.

Index categories: Transonic Flow; Nonsteady Aerodynamics; Computational Methods.

*Senior Research Associate. Member AIAA.
†Professor. Associate Fellow AIAA.

## Formulation

We write the unsteady small-disturbance equation for low-frequency transonic flows in the commonly used form

$$-2KM_\infty^2\phi_{xt}+\{1-M_\infty^2-(\gamma+1)M_\infty^2\phi_x\}\phi_{xx}+\phi_{yy}=0 \quad (1)$$

The spatial coordinates, the time, and the velocity potential in Eq. (1) have been nondimensionalized by the chord, the reciprocal of the angular frequency, and the freestream velocity times the chord, respectively. Other, perhaps more suitable, forms are given in Ref. 9. This equation results from a systematic expansion of the velocity potential in the thickness ratio $\tau$ and applies for reduced frequencies $K=O(\tau^{2/3})$, where $K=\omega c/U$, i.e., the angular frequency multiplied by the time it takes the flow to traverse the airfoil chord. Lin et al.[11] showed that, with restriction to small perturbations throughout the flow, Eq. (1) is the only nonlinear equation that arises. For moderate frequencies, the equation

$$-K^2M_\infty^2\phi_{tt}-2KM_\infty^2\phi_{xt}+\left\{1-M_\infty^2-(\gamma+1)M_\infty^2\times\left[\phi_x+\frac{\gamma-1}{\gamma+1}K\phi_t\right]\right\}\phi_{xx}+\phi_{yy}=0$$

frequently is used, with or without the $\phi_t$ term, and may provide results that apply at higher frequencies than those obtained from Eq. (1) or the linear form of the preceding equation.

Because $K=O(\tau^{2/3})$, the boundary condition on the body takes the simple form

$$\phi_y(x,0,t)=\tau[\partial Y(x,t)/\partial x+K\partial Y(x,t)/\partial t]$$
$$=\tau[Y_x^\circ+(\delta/\tau)(Y_x^u+KY_t^u)],\quad -\tfrac{1}{2}\le x\le\tfrac{1}{2} \quad (2)$$

where $Y(x,t)$, the instantaneous body shape, has been decomposed into a steady part $Y^\circ$ and an unsteady part $Y^u$. The last term, $KY_t^u$, is dropped except when $Y_x^u$ is small or zero because $K=O(\tau^{2/3})$. Here $\delta$ is the amplitude of the unsteady oscillation. Far from the body we require that the derivatives of $\phi$ vanish. In this approximation the pressure

coefficient, defined so that it vanishes at sonic conditions, takes the form

$$C_p = -2\left\{\frac{M_\infty^2 - 1}{(\gamma+1)M_\infty^2} + \phi_x\right\} \tag{3}$$

In the small-disturbance approximation, the Kutta condition is imposed by requiring that $C_p$ be continuous at $y=0$ for $x > 1/2$.

Any shock wave that exists in the flowfield must satisfy the jump relation derived from the conservative form of the governing equation, Eq. (1), namely,

$$-2KM_\infty^2 [\![ \phi_x ]\!]^2 \left(\frac{dx}{dt}\right)_s - \{1 - M_\infty^2 - (\gamma+1)M_\infty^2 \tilde{\phi}_x\} [\![ \phi_x ]\!]^2 + [\![ \phi_y ]\!]^2 = 0 \tag{4}$$

together with the condition derived from the assumption of irrotationality,

$$\left(\frac{dy}{dx}\right)_s = \frac{-[\![ \phi_x ]\!]}{[\![ \phi_y ]\!]} \tag{5}$$

Here $\tilde{\phi}_x$ refers to the mean value of $\phi_x$ evaluated on each side of the discontinuity, and $[\![ \phi_x ]\!]$ indicates the jump in $\phi_x$ across the discontinuity; the subscript $s$ denotes the quantity evaluated at the shock surface.

## Time-Linearized Equations

We now assume that the unsteady disturbances, characterized by $\delta$, are small enough so that we may write

$$\phi(x,y,t) = \phi^\circ(x,y) + \delta\psi(x,y,t) + o(\delta) \tag{6}$$

and neglect higher-order terms in $\delta$. The restriction imposed on $\delta$ for this to be true will depend on the other parameters of the problem, viz., $\kappa \equiv (1 - M_\infty^2)/[(\gamma+1)M_\infty^2\tau]^{2/3}$ and $K$. This gives

$$\{1 - M_\infty^2 - (\gamma+1)M_\infty^2 \phi_x^\circ\}\phi_{xx}^\circ + \phi_{yy}^\circ = 0 \tag{7a}$$

$$\phi_y^\circ(x,0) = \tau Y^{\circ\prime}(x), \quad -1/2 \le x \le 1/2 \tag{7b}$$

and

$$-2KM_\infty^2 \psi_{xt} + \{[1 - M_\infty^2 - (\gamma+1)M_\infty^2 \phi_x^\circ]\psi_x\}_x + \psi_{yy} = 0 \tag{8a}$$

$$\psi_y(x,0,t) = Y_x^u(x,t), \quad -1/2 \le x \le 1/2 \tag{8b}$$

The solution to Eqs. (7) must satisfy the steady version of the shock relations, Eqs. (4) and (5). The shock relations for Eqs. (8) are discussed later.

As mentioned previously, a shock-fitting scheme that approximates the shock waves as discontinuities normal to the freestream has been developed[9] with an alternating-direction implicit scheme (i.e., ADI) to compute the solution to Eq. (7). Comparison of these results with the results obtained[12] using an exact shock-fitting algorithm and line relaxation indicates that they should suffice for most studies. At the very least, they should prove adequate for the time-linearized studies of interest here, as only small shock excursions can be allowed.

We assume, then, that we have the numerical values for $\phi_x^\circ$ required in Eqs. (8). These data will be discontinuous across some vertical line, the shock wave, $x = x^*$, $0 \le |y| \le y^*$. We then ask, under what conditions are Eqs. (8) valid? And how do we account for shock wave motions in the linearized analysis? The answers to these questions are inferred from a simple one-dimensional model discussed in the next section.

Anticipating that we will wish to solve Eqs. (8) with the same technique that proved successful for Eq. (1), we avoid writing

$$\psi(x,y,t) = Re\{\bar{\psi}(x,y)e^{i\omega t}\} \tag{9}$$

Assumption (9) restricts the study to harmonic linear motions. Because indicial motions can be superimposed to obtain the results for any frequency, they too are important. Assumption (9) suppresses the time dimension of the calculation, but it results in two coupled equations, or one equation for a complex-valued $\bar{\psi}$, which may be solved by line relaxation. Our experience with unsteady ADI techniques has been that they are at least as effective as line relaxation for problems of this type, and hence there is no numerical advantage to the decomposition, Eq. (9). This conclusion also was arrived at by Ballhaus et al.[13] in a related study.

An appropriate scaling of the dependent and independent variables in Eqs. (7) and (8) allows either the thickness or the frequency to be normalized to the value 1, as expected. This scaling, in terms of the transonic similarity parameter $\kappa$, the amplitude of the unsteady motion $\delta$, its frequency $\omega$, and the body's basic thickness $\tau$, leads to

$$\psi(\tilde{x},\tilde{y};\kappa;\delta;\omega;1) = \omega\bar{\psi}\left(\tilde{x}, \frac{\tilde{y}}{\omega^{1/2}}; \frac{\kappa}{\omega^{1/2}}; 1; \frac{1}{\omega^{1/2}}\right)$$

where $\tilde{x}$ and $\tilde{y}$ are suitably scaled replacements for the $x$ and $y$ coordinates. This result can be used to check trends noted in the numerical results.

## One-Dimensional Model

To answer the questions just raised, we study a simple unsteady one-dimensional analog of Eq. (2). We consider a one-dimensional unsteady equation that models the important features of Eq. (2), and ascertain how a simple steady solution is modified by small unsteady perturbations. We consider, then,

$$2\phi_{xt} + (1 - \phi_x)\phi_{xx} = 2\phi_{xt} - 1/2\{(1 - \phi_x)^2\}_x = 0 \tag{10}$$

subject to $\phi(0,t) = f_1(t)$, $\phi_x(0,t) = f_2(t)$, and either $\phi(1,t)$ or $\phi_x(1,t) = f(t)$. There are restrictions on $f$ which, for brevity, we do not list. Our study could be generalized by replacing $1 - \phi_x$ in Eq. (10) by $[A(x) - \phi_x]$, where $A(x)$ is a continuous function of $x$, but little added insight is gained.

To simplify matters further, consider the especially simple subcase $f_1 = 0$, $f_2 = -1$, $f = 3 + \delta p(t)$. When $\delta \equiv 0$, we have the steady solution

$$\phi^\circ = \begin{cases} -x, & 0 \le x \le 3/4 \\ -3(1-x), & 3/4 \le x \le 1 \end{cases}$$

This satisfies Eq. (10) and the jump condition that one derives from it, viz.,

$$[\![ \phi ]\!] = 0 \text{ on } 2\frac{dx_s}{dt} = 1 - \tilde{\phi}_x \tag{11}$$

Now a general solution of Eq. (10), in terms of $\phi_x$, is

$$\phi_x = \text{arbitrary function of } \left(t + \frac{2(1-x)}{1-\phi_x}\right)$$

This can be verified by substitution. With, say $v_x(1,t) = 3 + \delta p(t)$, we have, for $x > x_s$,

$$\phi(x,t) = 3(x - x_s) + \delta\int_{x_s}^{x} p\left(t + \frac{2(1-\hat{x})}{1 - \phi_x(\hat{x},t)}\right)d\hat{x} - h(t) \tag{12}$$

where the choice $h(t)=x_s(t)$ insures that $[\![\phi]\!]=0$ at $x=x_s$ because $\phi=\phi^\circ$ for $x<x_s$.

The shock motion must be determined by the direct integration of Eq. (11):

$$2\frac{dx_s}{dt}=1-\tilde{\phi}_x=-\frac{\delta}{2}p[x_s(t),t] \tag{13}$$

Now, for comparison, we determine the results that are obtained by time linearization; i.e., we write

$$\phi(x,t;\delta)=\phi^\circ(x)+\delta\psi(x,t)+o(\delta) \tag{14}$$

and solve the linear equation for $\psi$ which results by dropping higher-order terms in $\delta$. That is, we solve

$$2\psi_{xt}+(1-\phi_x^\circ)\psi_{xx}-\phi_{xx}^\circ\psi_x=0 \tag{15}$$

subject to $\psi_x(1,t)=p(t)$.

We now linearize the first of Eqs. (11) as follows:

$$[\![\phi(x,t)]\!]=0=[\![\phi(x_s^\circ,t)+\phi_x(x_s^\circ,t)[x_s(t)-x_s^\circ]+\ldots]\!]$$

$$=[\![\phi^\circ(x_s^\circ)+\delta\psi(x_s^\circ,t)+\phi_x^\circ[x_s(t)-x_s^\circ]]\!]$$

Thus we conclude that

$$\delta[\![\psi(x_s^\circ,t)]\!]=-[\![\phi_x^\circ(x_s^\circ)]\!](x_s-x_s^\circ) \tag{16}$$

From the second of Eqs. (11), with $x_s(t)=x_s^\circ+\delta\chi(t)$, we find

$$\frac{d\chi}{dt}=-\frac{1}{2}\tilde{\psi}_x=-\frac{1}{4}\psi_{x_b}$$

where $(\,)_b$ refers to the value behind the shock. Thus we may replace Eq. (11) by

$$[\![\psi(x_s^\circ,t)]\!]=-[\![\phi_x^\circ(x_s^\circ)]\!]\chi$$

or

$$\psi_b(x_s^\circ,t)=-4\chi(t) \tag{17a}$$

and

$$\frac{d\chi}{dt}=-\frac{1}{4}\psi_{x_b} \tag{17b}$$

**Example**

Consider now, for example, $p(t)=\sin\omega t$; it is easy to show that a general solution to Eq. (15) is

$$\psi(x,t)=-(1/\omega)[\cos\omega(1-x-t)-h(t)]$$

The function $h(t)$ follows from Eqs. (17a) and (17b) and assuming, e.g., that $\psi(\frac{3}{4},0)=0$. Thus,

$$\psi(x,t)=-(1/\omega)[\cos\omega(1-x-t)-\cos(\omega/4)] \tag{18}$$

and

$$\chi(t)=(1/4\omega)[\cos\omega(\tfrac{1}{4}-t)-\cos(\omega/4)] \tag{19}$$

Had we solved Eq. (15) with $\psi\equiv0$ for $x<x_s(t)$ and determined the exact shock motion from Eq. (11) with $1-\phi_x=-2+O(\delta)$ used in Eq. (12), we would find that behind the shock

$$\phi(x,t)=\phi^\circ+3-4x_s-(\delta/\omega)[\cos\omega(1-x-t)$$

$$-\cos\omega(1-x_s-t)] \tag{20}$$

where the shock motion is given explicitly by

$$x_s=\frac{2}{\omega}\tan^{-1}\left\{\frac{\tan\frac{\omega}{2}(t+c)-\left[\tan\frac{\omega}{2}(t-1)-\frac{\delta}{4}\right]}{1+\tan\frac{\omega}{2}(t-1)\left[\tan\frac{\omega}{2}(c+t)+\frac{\delta}{4}\right]}\right\} \tag{21}$$

with $c=-2(\tan^{-1}[\tan(\omega/8)+\delta/4])/\omega$. For $\omega\gg\delta$, which is required for small shock motions, Eq. (21) simplifies to

$$x_s=\tfrac{3}{4}+(\delta/4\omega)[\cos\omega(\tfrac{1}{4}-t)-\cos(\omega/4)]$$

Thus these results are in agreement with Eqs. (18) and (19) to lowest order in $\delta$.

The time-linearized results, Eqs. (18) and (19), now are compared with the exact results. The nonlinear result for $x>x_s$, given by Eqs. (12) and (13), is

$$\phi=\phi^\circ+3-4x_s(t)+\delta\int_{x_s}^{x}\sin\omega\left(t+\frac{2(1-\hat{x})}{1-\phi_x(\hat{x},t)}\right)d\hat{x} \tag{22}$$

where

$$\frac{dx_s}{dt}\equiv\dot{x}_s=-\frac{\delta}{4}\sin\omega\left(t+\frac{1-x_s}{1-2\dot{x}_s}\right) \tag{23}$$

The results, Eqs. (22) and (23), are consistent with the time-linearized results, Eqs. (18) and (19), to $O(\delta)$, except for a slow secular drift in the shock position of $O(\delta^2 t)$ that occurs in Eq. (23) but not in Eq. (19). This is an artifact of our one-dimensional model; even if it were not, it would not invalidate the use of the linear results for flutter studies where $\delta$ is small and structural damping determines the time scale of interest.

The main conclusions that we derive from this study are that it is essential to consider shock motion in computing time-linearized solutions if we are to determine the effects of small unsteady perturbations correctly to lowest order, and that shock excursions increase as the frequency is decreased. Additionally, this motion can be computed in a straightforward manner.

## Two-Dimensional Time-Linearized Analysis

The results from our simple model show that the time-linearized results must be corrected for shock motion if they are to be consistently correct to lowest order. This can be accomplished by calculating the shock motion in conjunction with the time-linearized solution. Here we follow an analogous procedure and calculate the change with time of the values of the perturbed potential behind the shock required by the linearized shock jump relations. Thus, we wish to solve Eq. (8a) with Eq. (8b) subject to the far-field boundary and Kutta conditions. As we noted, the steady result for $\phi_x^\circ$ can be calculated adequately for most small-disturbance flows using normal shock fitting, as described in Ref. 9. Under the assumption that the shock wave is normal, the shock jump conditions, Eqs. (4) and (5), can be replaced by requiring

$$[\![\phi]\!]=0 \text{ on } \frac{dx_s}{dt}=\frac{\gamma+1}{2K}\left\{\frac{M_\infty^2-1}{(\gamma+1)M_\infty^2}+\tilde{\phi}_x\right\} \tag{24}$$

For steady flow, $\dot{x}_s=0$ and in Eq. (24) $\{\cdots\}=0$. We express the shock positon as

$$x_s=x_s^\circ+\delta\chi(t)$$

and conclude that the shock motion is governed by

$$\frac{d\chi}{dt}=\frac{\gamma+1}{2K}\tilde{\psi}_x$$

As discussed in Ref. 9, $\tilde{\psi}_x$ is evaluated at $y=0$. On the shock

$$[\![\phi]\!] = [\![\phi^\circ]\!] + \delta [\![\psi]\!] \tag{25}$$

Linearizing Eq. (25) for the velocity potential about the steady shock position, we find

$$\phi(x_s,y,t) = \phi(x_s^\circ,y,t) + \phi_x(x_s^\circ,y,t)\delta\chi$$

$$= \phi^\circ(x_s^\circ,y) + \phi_x^\circ(x_s^\circ,y)\delta\chi + \delta\psi(x_s^\circ,y,t) + O(\delta^2)$$

Because we have treated the shock as a normal one, $y$ appears here simply as a parameter. Now $[\![\phi(x_s,y,t)]\!]$ and $[\![\phi^\circ(x_s^\circ,y)]\!]$ are both zero; consequently, we have

$$[\![\psi(x_s^\circ,y,t)]\!] = -\frac{(\gamma+1)}{2K}[\![\phi_x^\circ(x_s^\circ,y)]\!]\int_0^t \tilde{\psi}_x(x_s^\circ,0,\hat{t})\,d\hat{t} \tag{26}$$

which must be integrated in time in conjunction with the solution to Eq. (8).

Equation (8) now is solved numerically in time and space in conjunction with Eq. (26), which is used to update the values of $\psi$ behind the shock. We start with a steady solution and initiate a body motion, such as the harmonic oscillation of a flap. The calculations proceed in time until they are judged to be periodic. Note that indicial as well as harmonic motions may be considered because we have not utilized the usual harmonic decomposition, Eq. (9).

## Numerical Procedure

The numerical procedure used here derives from that developed for the nonlinear equation, Eq. (1). The main simplification occurs in the shock jump conditions. In order to minimize the far-field boundary effects on the results which, as Magnus[14] has noted, can be significant, we again use coordinate stretching[9] in the form

$$\xi = \pm[1-\exp(-a_1|x|)] \quad \text{for } x \gtrless 0$$

$$\eta = \pm[1-\exp(-a_2|y|)] \quad \text{for } y \gtrless 0$$

where $a_1$ and $a_2$ are constants that determine the mesh distribution. This stretching transforms the infinite physical domain into a computational domain bounded by $|\xi| \le 1$ and $|\eta| \le 1$. The mesh distribution is concentrated on the airfoil. In these coordinates, Eq. (8) becomes

$$A_1\{\psi_\xi\}_t + A_2\{f(\xi,\eta)(1-|\xi|)\psi_\xi\}_\xi + A_3\{(1-|\eta|)\psi_\eta\}_\eta = 0 \tag{27}$$

where

$$A_1 = \frac{-2KM_\infty^2 a_1}{a_2(1-|\eta|)}, \quad A_2 = \frac{a_1^2}{a_2(1-|\eta|)}, \quad A_3 = \frac{a_2}{1-|\xi|}$$

and

$$f(\xi,\eta) = 1 - M_\infty^2 - a_1(\gamma+1)M_\infty^2(1-|\xi|)\phi_\xi^\circ$$

is known in discrete form from the steady numerical solution. This function is discontinuous at $\xi = \xi_s^\circ$ for $0 \le |\eta| \le \eta^*$. First-order backward time and spatial differences are used for the first term. Centered or first-order backward differences are used for the second term if $f$ is less than or greater than zero, respectively; $f(\xi,\eta)$ is known in advance, with the derivative $\phi_\xi^\circ$ automatically evaluated correctly. Centered differences are used for the third term and denoted by $\delta_\eta$.

The solution is computed using an alternating-direction implicit procedure first applied to transonic flow problems by Ballhaus and Steger[15] and by Beam and Warming,[16] and subsequently refined further by Ballhaus and Goorjian.[17] The solution is advanced in time from its initial steady state to subsequent time levels with the following two-step procedure.

New values of $\psi$, denoted by $\psi^+$, are calculated along $\eta = \text{const}$ lines using

$$A_1\frac{\psi_\xi^+ - \psi_\xi^n}{\Delta t} + A_2\{f(\xi,\eta)(1-|\xi|)\psi_\xi^+\}_\xi$$

$$+ A_3\delta_\eta\{(1-|\eta|)\psi_\eta^n\} = 0$$

This is coupled with the computation of new values of $\psi^+$ behind the shock obtained by using Eq. (26). With the shock located at $\xi_s^\circ$ such that $\xi_s < \xi_s^\circ < \xi_{s+1}$, we can express the values of $\psi$ ahead of and behind the shock in a Taylor series, finally arriving at the result

$$[\![\psi]\!]^+ = -C(\eta)\Delta t\tilde{\psi}_\xi^n + [\![\psi]\!]^n \tag{28}$$

where

$$C(\eta) = [(\gamma+1)/4K]a_1^2(1-|\xi_s^\circ|)^2[\![\phi_\xi^\circ(\xi_s^\circ,\eta)]\!]$$

and $\tilde{\psi}_\xi^n$ is evaluated, following Eq. (26), at $\eta = 0$. One-half the change in $\psi$ across the shock is accounted for in this step, effectively using the trapezoidal rule in the time integration, Eq. (26); hence $C$ is half the value implied by Eq. (26).

With the values of $\psi^+$ determined, the new values of $\psi$ at the subsequent time level, $\psi^{n+1}$, are calculated using

$$A_1\frac{\psi_\xi^{n+1} - \psi_\xi^+}{\Delta t} + \frac{A_3}{2}\delta_\eta\{(1-|\eta|)(\psi_\eta^{n+1} - \psi_\eta^n)\} = 0$$

in conjunction with the completion of the time integration, Eq. (26):

$$[\![\psi]\!]^{n+1} = -C(\eta)\Delta t\tilde{\psi}_\xi^{n+1} + [\![\psi]\!]^+ \tag{29}$$

Again, $\tilde{\psi}_\xi^{n+1}$ is evaluated at $\eta = 0$.‡

The full procedure is, effectively,

$$A_1[(\psi_\xi^{n+1} - \psi_\xi^n)/\Delta t] + A_2\{f(\xi,\eta)(1-|\xi|)\psi_\xi^+\}_\xi$$

$$+ \tfrac{1}{2}A_3\delta_\eta\{(1-|\eta|)(\psi_\eta^{n+1} + \psi_\eta^n)\} = 0$$

with Eq. (26) implemented in the form of Eqs. (28) and (29). The procedure outlined here effectively corrects the $\psi$ values for shock motions as the solution progresses. The shock motion is easily determined simultaneously by using Eq. (26) and the expression for $d\chi/dt$ to find

$$\chi^{n+1}(0,t) = -[\![\psi(x_s^\circ,0,t)]\!]^{n+1} / [\![\phi_x(x_s^\circ,0)]\!] \tag{30}$$

The computations then provide results for $\phi_x$ like those sketched in Fig. 1. This figure depicts the steady-state result and the unsteady changes, as well as the shock positions at two different time levels where the shock is behind the steady-state position. When the shocks have been inserted in their known positions, we see that we need to continue data analytically ahead of and behind the shock in order to complete the solution. For shock excursions that are $o(1)$, we simply can extrapolate the steady-state data, both ahead of and behind the shock, to determine the pressure distribution on the body correctly to lowest order. Larger shock motions are, of course, not admissable in this theory.

‡The results given by the authors in Ref. 18 were in error because $\tilde{\psi}_\xi$ was allowed to vary with $\eta$; this is not consistent with the normal shock approximation that gives Eq. (24).

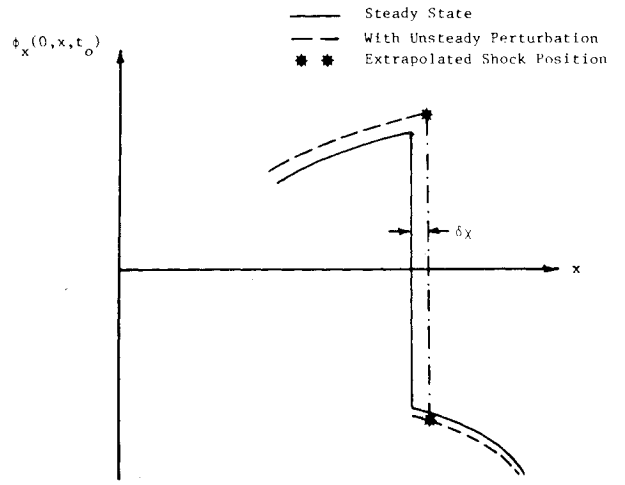


**Fig. 1 Sketch of steady state $\phi_x$, effect of perturbation $\delta\psi_x$, and resulting shock excursion.**

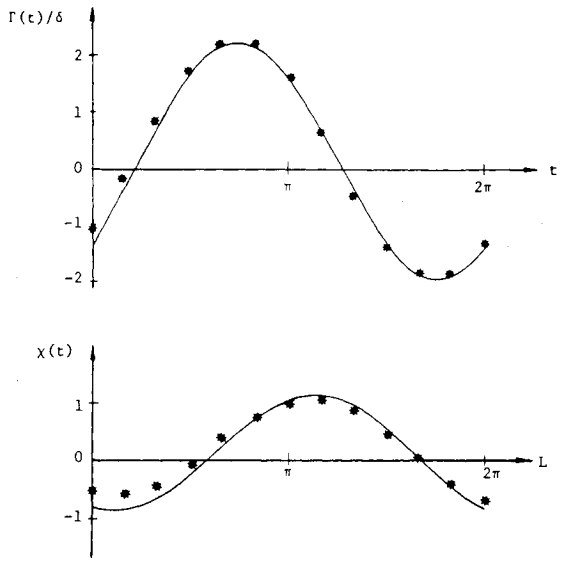


**Fig. 2 Nonlinear (***) and time-linearized (———) circulation and shock position for the pitching motion of an NACA 64A006 airfoil. Results shown are for the fifth cycle. The nonlinear results are for $\delta = 0.1$ deg and are not yet periodic ($M_\infty = 0.880$, $K = 0.48$).**

## Results and Discussion

Time-linearized results have been computed for an NACA 64A006 airfoil experiencing harmonic pitching and flap motions. As noted earlier, in the low-frequency approximation made here, pitching and plunging motions lead to the same result except that the time-linearized perturbations are proportional to the maximum pitch angle for the former, and $K$ times the maximum amplitude for the latter. Harmonic motions initiated from a steady state become nearly periodic in three to ten cycles, with the changes induced by flap oscillations becoming periodic more rapidly than those resulting from pitching oscillations. More cycles were required for larger frequencies and, to a lesser degree, higher Mach numbers.

In order to confirm the validity of the time-linearized calculations, both the time-linearized and nonlinear algorithms were used to compute the response to a step change in angle of attack and the harmonic response to pitching motions. Figure 2 compares the nonlinear and time-linearized results for the normalized circulation and shock position for harmonic pitching motions at $M_\infty = 0.88$ and $K = 0.48$. For these conditions, very small unsteady changes lead to very

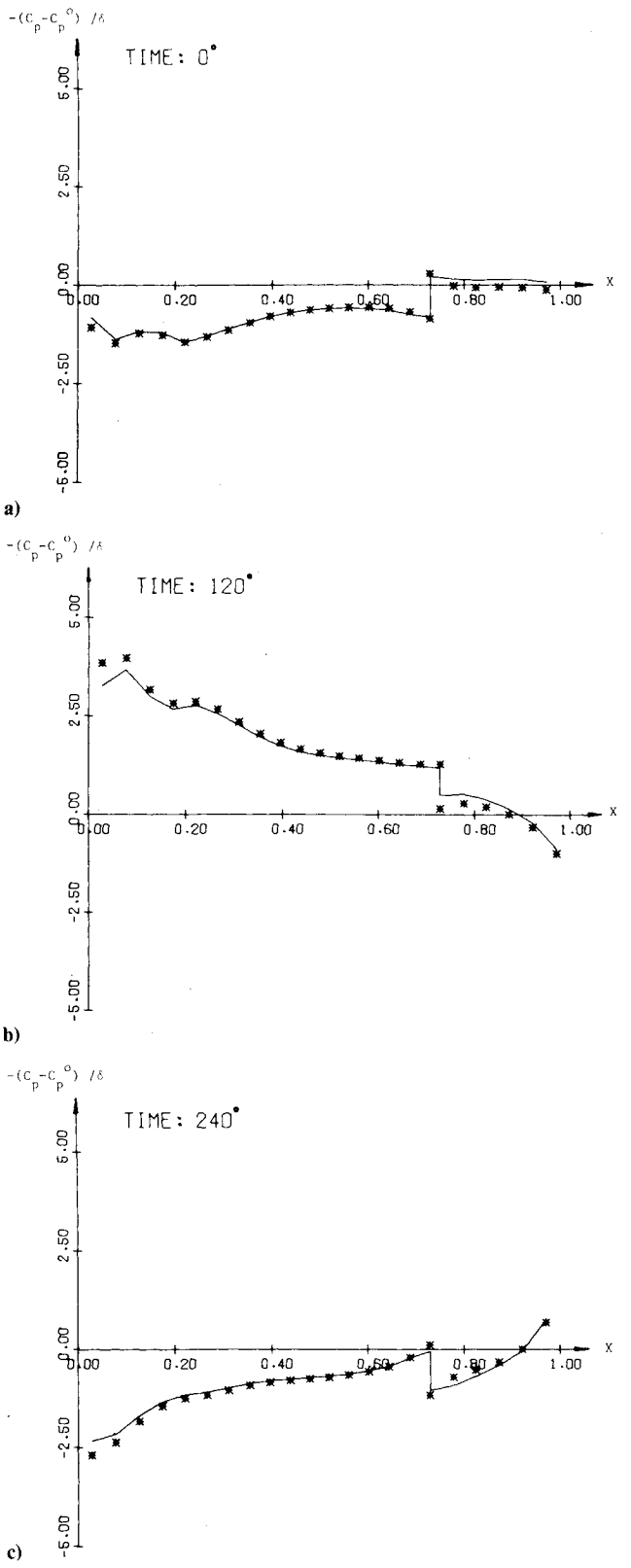


**Fig. 3 Normalized nonlinear (***) and time-linearized (———) pressure perturbations on the upper surface of an NACA 64A006 at three times. Pitching motion with $M_\infty = 0.880$, $K = 0.48$. For the nonlinear calculations, $\delta = 0.1$ deg.**

small shock motions, and in both calculations the shock wave remains between grid points. Because of the extrapolation procedure used in the nonlinear shock-fitting, the finite mesh size used can introduce errors, albeit small ones, in the shock's position when a grid line is crossed. We wished to eliminate these errors in order to use the nonlinear

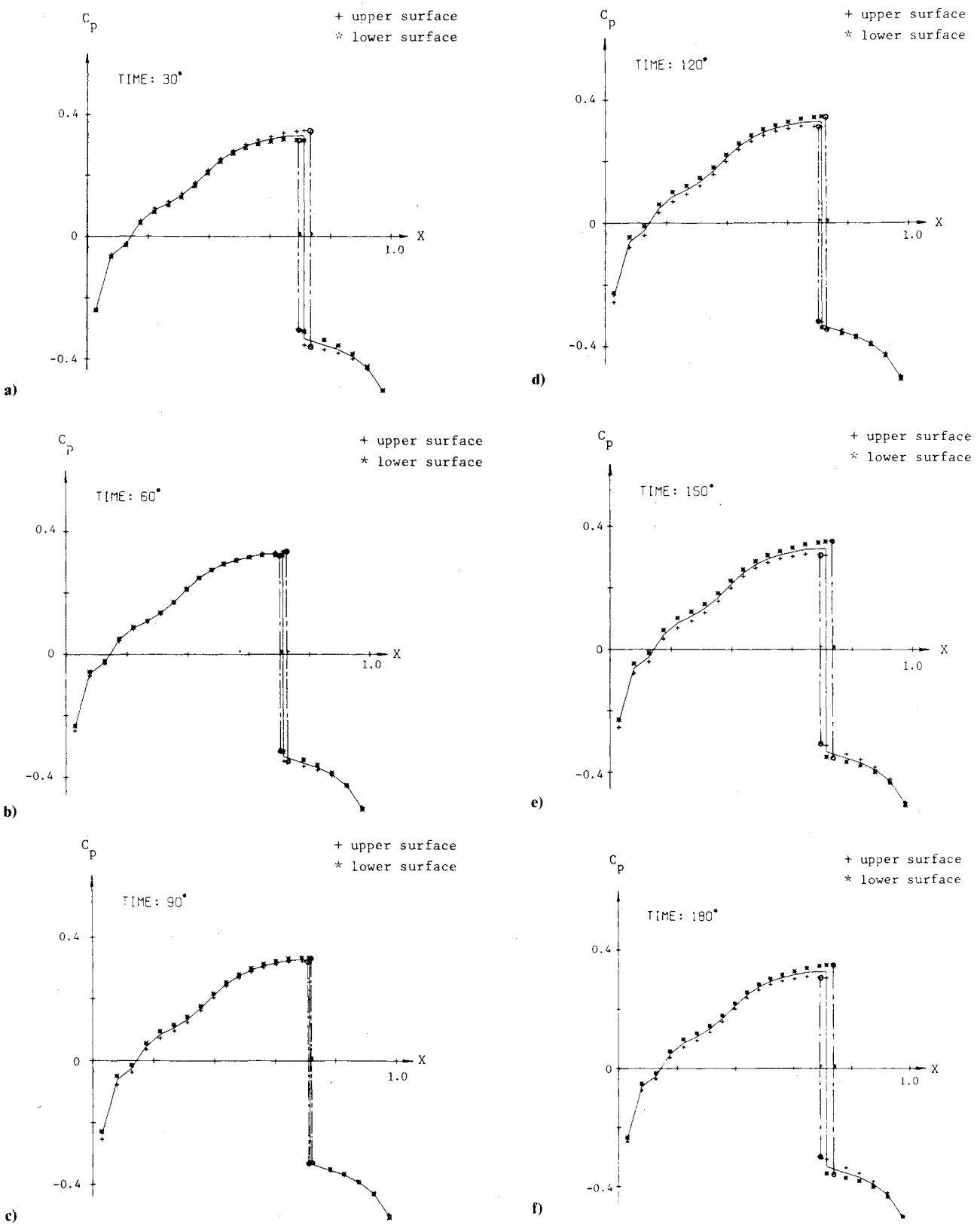


**Fig. 4 Time-linearized pressure coefficients on the upper (+) and lower (*) surfaces on an NACA 64A006 airfoil with oscillating quarter-chord flap ($M_\infty = 0.875$, $K = 0.06$, $\delta = 0.25$ deg).**

calculations to judge the accuracy of time-linearized calculations. These results indicate that for pitching about midchord, nonlinear, amplitude-dependent behavior occurs for $\delta/\tau \geq 0.1$ for $K = 0.48$. Because the amplitude of the shock motion increases with decreasing $K$, nonlinear effects occur at smaller values of $\delta/\tau$ at lower reduced frequencies. Results are given for the fifth cycle; note that the nonlinear results are not yet periodic. Figure 3 compares the nonlinear and time-linearized pressure deviation from steady state at three angular times for the same conditions. Good agreement between the results is obtained for $\delta/\tau$ less than 0.1.

Time-linearized pressure distributions at six angular positions for an oscillating quarter-chord flap with $K = 0.06$ and $M_\infty = 0.875$ are shown in Fig. 4. The flap deflection is

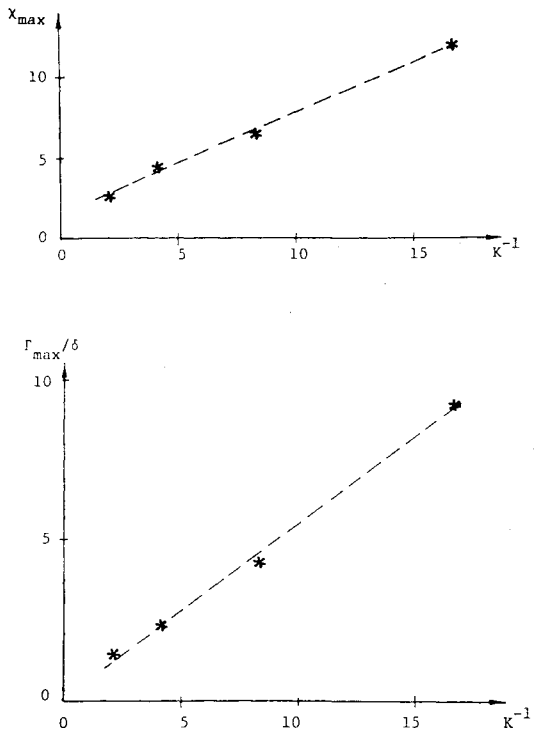


**Fig. 5 Normalized maximum shock excursion and circulations as a function of inverse reduced frequency for an NACA 64A006 airfoil with oscillating quarter-chord flap ($M_\infty = 0.875$).**

downward during the first half of the cycle. The results for the second half of the period, for the symmetrical problem shown here, are just the results shown with the lower and upper surface pressures interchanged. Thus the results for 0 deg are not given, as they are just those for 180 deg with the lower and upper surface pressures reversed. Because the flap hinge occurs very close to the steady-state shock location, the pressure singularity due to the change in flow direction at the hinge is missed. The circulation and shock excursion obey the following relations:

$$\Gamma(t)/\delta = 9.26 \sin(t - 59 \text{ deg})$$

$$\chi(t) = 12 \sin(t - 51 \text{ deg})$$

Note the substantial phase lag in the circulation and the shock's position.

Time-linearized pressure distributions for an oscillating airfoil with $K = 0.12$ and $M_\infty = 0.875$ also were computed. The results, if multiplied by $K$, represent the pressure perturbations for a plunging airfoil. As in the previous case of an oscillating flap, changes in forces and moments of $O(\delta/K)$ occur due to shock wave motion. In this case,

$$\Gamma(t)/\delta = 5.48 \sin(t - 70 \text{ deg})$$

$$\chi(t) = 5.62 \sin(t - 87 \text{ deg})$$

Analogous computations have been carried out for $K = 0.06$, 0.12, 0.24, and 0.48. Figure 5 depicts the shock wave's excursion and maximum circulation as a function of $K^{-1}$. The nearly linear variation of the shock excursion substantiates an observation made in a one-dimensional model where the shock wave excursion is directly proportional to $1/K$.

In these calculations the circulation gives an immediate evaluation of the lift coefficient as a function of time; the moment coefficient must be evaluated by integrating the moment of the pressure coefficient. This is done by integrating the moment of pressure perturbations with the shock wave in its steady-state position and then correcting these results for the moment due to the shock wave motion, assuming that the shock's strength is defined by the steady-state pressure field. This makes an error in the shock strength of $O(\delta)$, but the effect on the moment is $O(\delta^2/K)$; because we have neglected other higher-order terms, it is consistent to neglect this change in the strength of the shock wave.

For the time-linearized results to be valid, we must really require $\delta/\tau K \ll 1$. Our numerical results indicate that, for $\delta/\tau K \leq 0.2$, the unsteady perturbations are essentially linear.

The time-linearized algorithm used here is a derivative of that used for the nonlinear calculations. Consequently, computational times are not greatly reduced from those required for the nonlinear calculations. The linearity of these computations may make it possible to greatly reduce the computational effort required. Numerical experience has shown some difficulties for $\Delta t$ (deg)$/K \geq 50$. This is in agreement with the consistency requirement for thg ADI algorithm used here. Both the domain-of-dependence condition and a local linearized stability analysis show the procedure to be unconditionally stable. Each time step requires about 2 s of CPU time on a CDC 6400, or about 0.1 s on a CDC 7600. The number of time steps required for a given computation is somewhat less than that required for the nonlinear computations at small values of $K$, and comparable at larger values of $K$.

## Conclusion

An accurate and efficient procedure for computing time-linearized, small-perturbation, low-frequency transonic flows, including shock wave motions, has been developed. Shock motions must be included, as their amplitude is proportional to that of the motion divided by the reduced frequency. Both indicial and harmonic responses for various modes of motion may be computed in seconds on a CDC 7600.

## Acknowledgement

This research was sponsored by the Air Force Office of Scientific Research through Grant 76-2954E and the Office of Naval Research through Grant N0014-76-C-0182.

## References

[1] Ballhaus, W. F., "Some Recent Progress in Transonic Flow Computations," *VKI Lecture Series on Computational Fluid Dynamics*, von Kármán Institute for Fluid Dynamics, Rhode-St-Genese, Belgium, March 15-19, 1976.

[2] Landahl, M. T., *Unsteady Transonic Flow*, Pergamon Press, New York, 1961.

[3] Tijdeman, H., "Remarks on the Transonic Flow Around Oscillating Airfoils," *AGARD Fluid Dynamics Panel Symposium on Unsteady Aerodynamics*, Paper 227-10, Ottawa, Canada, 1977.

[4] Traci, R. M., Albano, E. D., and Farr, J. L., Jr., "Perturbation Method for Transonic Flow about Oscillating Airfoils," AIAA Paper 75-877, 1975.

[5] Weatherill, W. A., Ehlers, F. E., and Sebastian, J. D., "Computation of the Transonic Perturbation Flow Field Around Two- and Three-Dimensional Oscillating Wings," NASA CR-2599, 1975.

[6] Ehlers, F. E., "A Finite Difference Method for the Solution of the Transonic Flow About Harmonically Oscillating Wings," NASA CR-2257, 1974.

[7] Tijdeman, H., "On the Motion of Shock Waves on an Airfoil with Oscillation Flap in Two-Dimensional Transonic Flow," NLR TR 75038U, 1975.

[8] Tijdeman, H., "On the Motion of Shock Waves on an Airfoil with Oscillating Flap," *IUTAM Symposium Transsonicum II*, edited by K. Oswatitsch and D. Rues, Göttingen, 1975, pp. 49-56.

[9] Yu, N. J., Seebass, A. R., and Ballhaus, W. F., "An Implicit Shock-Fitting Scheme for Unsteady Transonic Flows Computations," AIAA Paper 77-633, 1977; also *AIAA Journal*, Vol. 16, July 1978, pp. 673-678.

[10] Nixon, D., "Perturbation of Discontinuous Transonic Flow," *AIAA Journal*, Vol. 16, Jan. 1978, pp. 47-52.

[11] Lin, C. C., Reissner, E., and Tsien, H. S., "On Two-Dimensional Non-Steady Motion of a Slender Body in a Compressible Fluid," *Journal of Mathematics and Physics*, Vol. 27, No. 3, 1948, pp. 220-231.

[12] Yu, N.J. and Seebass, R., "Accuracy of Transonic Flow Computations" (unpublished), 1977.

[13] Ballhaus, W. F., Jameson, A., and Albert J., "Implicit Approximate-Factorization of Steady Transonic Flow Problems," NASA TM X-73202, 1977.

[14] Magnus, R. J., "Computational Research on Inviscid, Unsteady, Transonic Flow over Airfoils," Office of Naval Research, Rept. CASD/LVP 77-010, 1977.

[15] Ballhaus, W. F. and Steger, J. L., "Implicit Approximate-Factorization Schemes for the Low-Frequency Transonic Equation," NASA TM X-73082, 1975.

[16] Beam, R. M. and Warming, R. F., "An Implicit Finite-Difference Algorithm for Hyperbolic Systems in Conservation-Law Form," *Journal of Computational Physics*, Vol. 22, Jan. 1976, pp. 87-110.

[17] Ballhaus, W. F. and Goorjian, P. M., "Implicit Finite Difference Computations of Unsteady Transonic Flows about Airfoils, Including the Treatment of Irregular Shock Wave Motions," *AIAA Journal*, Vol. 15, Dec. 1977, pp. 1728-1735.

[18] Fung, K.-Y., Yu, N. J., and Seebass, R., "Small Unsteady Perturbations in Transonic Flows," AIAA Paper 77-675, Albuquerque, N. Mex., June 1977.